J. Phys. D: Appl. Phys., **16** (1983) 1673–1685. Printed in Great Britain

Modelling of a low-pressure plasma column sustained by a surface wave

C M Ferreira†

Laboratoire de Physique des Gaz et des Plasmas‡, Université de Paris-Sud, 91405 Orsay, France

Received 25 February 1983

Abstract. A complete theoretical description of a low-pressure, cylindrical plasma column sustained by a weakly damped surface wave is derived in which the equations describing the steady-state plasma maintenance conditions are coupled with the surface wave propagation and attenuation characteristics. The present formulation extends a radial theory of the maintenance of the plasma column previously reported to include the axial variation in the radially averaged plasma properties. Simple similarity laws for this type of discharge are proved to exist under quite general conditions. Analytic expressions are derived for the variation of the electron density along the discharge axis and for the length of the plasma column as a function of the operating parameters. The calculations are shown to agree well with available experimental data.

1. Introduction

The properties of plasma columns produced and sustained by surface microwaves have been investigated in recent years by various authors, both theoretically and experimentally (Moisan *et al* 1975, Zakrzewski *et al* 1977,Moisan *et al* 1979a, b, Glaude *et al* 1980, Moisan *et al* 1980, Ferreira 1981, Nghiem *et al* 1982, Chaker *et al* 1982, Aliev *et al* 1982). These studies have shown that surface wave produced plasmas can be used with some advantage to replace other more conventional plasma sources, e.g., DC discharges and other kinds of microwave produced plasmas, for such important applications as plasma chemistry, laser excitation, spectroscopic sources, plasma etching, etc. The principal properties and applications of this kind of plasma have recently been reviewed by Moisan *et al* (1982).

Although some theoretical work has been devoted, in recent years, to the understanding of the surface wave propagation characteristics and the plasma maintenance mechanisms, a complete, satisfactory theoretical description is not yet available. Calculations of the surface wave dispersion characteristics, attenuation coefficient and electric and magnetic field radial profiles have been reported (Zakrzewski *et al* 1977, Chaker *et al* 1981, Nghiem *et al* 1982) for the case of a weakly damped ($\omega \gg \nu_c$, where ω is the wave angular frequency and ν_c is an effective electron–neutral collision frequency

† Permanent address: Centro de Electrodinâmica da Universidade Técnica de Lisboa, Instituto Superior Técnico, 1096 Lisboa Codex, Portugal.

‡ Laboratory associated with the CNRS.

for momentum transfer) surface wave propagating along a radially homogeneous, cold (thermal velocity $\ll$ phase velocity) plasma column. The axial electron density distributions observed in the experiments were also successfully explained in terms of a semi-empirical model which assumes that the wave power absorbed over a given axial length of plasma column is proportional to the total number of electrons in that slice and independent of the incident wave power (Glaude *et al* 1980, Chaker *et al* 1982). Another theory which is based on quite a different point of view, i.e., that of the maintenance of the plasma column, was developed by Ferreira (1981, hereafter referred to as I). The formulation of this theory is based on the continuity and momentum transfer equations for the electrons and ions, which are coupled to the equations describing the radial variation of the wave electric field inside the plasma through the electron power balance equation. Therefore, the mutual influence of the wave field and plasma density radial profiles on each other are treated self-consistently. However, this work was only concerned with radial variations in the different physical quantities of interest and axial variations were not investigated.

It is the purpose of the present work to extend the formulation given in paper I to include axial variations as well, thus providing a complete physical description of the surface wave produced plasma column. As in I, only the low-attenuation regime (i.e., $\omega \gg \nu_c$) will be considered here. Comparison of theory with experiments in argon shows that the present formulation yields accurate predictions of the axial electron density distribution and of the length of the plasma column as a function of the various operating parameters, i.e., gas pressure, wave frequency and incident power, and discharge tube radius.

2. Theoretical formulation

The experimental situation to be considered here is similar to that described in paper I. An azimuthally symmetric surface wave (a TM wave in which the electric and magnetic field components are E_z, E_r and H_φ, respectively, where r, φ, and z are the radial, azimuthal and axial cylindrical coordinates) is launched by a surfatron and propagates with wave-vector $\beta + j\alpha$ along z; $\beta(=2\pi/\lambda)$ and α are the wavenumber and the attenuation coefficient, respectively. This wave creates and sustains a plasma column in a cylindrical Pyrex glass tube. Let a, b, and d denote the inside and outside radii of the discharge tube and the inside radius of the outer metallic waveguide, respectively (for a schematic of a typical experimental apparatus see figure 1 in Nghiem *et al* 1982).

With regard to wave propagation under low attenuation conditions, the plasma may be described as dielectric medium of relative permittivity

$$\varepsilon_p = 1 - (\omega_{pe}/\omega)^2 \tag{1}$$

where $\omega_{pe} = (n_e e^2/\varepsilon_0 m)^{1/2}$ is the electron plasma angular frequency. Here n_e, e and m are the electron density, charge and mass, respectively, and ε_0 is the vacuum permittivity. Surface waves can only propagate in this system provided $\omega < \omega_{pe}/(1 + \varepsilon_g)^{1/2}$, where ε_g is the discharge tube relative permittivity.

A complete, fully self-consistent theory of this system could be formulated using the full set of Maxwell equations in the three media (i.e., the plasma, the glass tube and the outer space), with the appropriate boundary conditions for the wave fields at the various interfaces, together with the equations describing the balancing between the creation and the loss of the electrons and ions in the plasma (see I). Unfortunately, owing to the plasma inhomogeneity in both the radial and axial directions, this set of equations is

quite intractable and of limited practical use. As a first approximation however one can neglect the effects of the plasma radial inhomogeneity on the surface wave propagation characteristics and split up the basic set of equations into two uncoupled sets. (i) On one hand consider the Maxwell equations and the boundary conditions for the fields, assuming a radially homogeneous plasma of relative permittivity $\bar{\varepsilon}_p = 1 - (\bar{\omega}_{pe}/\omega)^2$, where $\bar{\omega}_{pe}$ is the electron plasma angular frequency corresponding to the radially averaged electron density $\bar{n}_e$. From these equations the surface wave dispersion and attenuation characteristics can readily be obtained (Chaker *et al* 1981, Nghiem *et al* 1982). (ii) On the other hand consider the radial equations describing the plasma maintenance mechanisms, given in paper I. Such a formulation constitutes a complete, though approximate, physical description enabling the determination of $\bar{n}_e(z)$ and of the length of the plasma column as a function of the operating parameters. (The radial variations in the different physical quantities of interest were studied in I and need not be further considered here.)

2.1. Dispersion and attenuation characteristics. Axial distribution of the electron density

We briefly summarise in this section the results deduced by several workers (Glaude *et al* 1980, Chaker *et al* 1981, 1982, Nghiem *et al* 1982) for the case of a weakly damped surface wave propagating along a radially homogeneous cold plasma column. From the Maxwell equations and the boundary conditions for the fields the surface wave wavenumber β and the field radial profiles can be determined uniquely as a function of ω, $\bar{\omega}_{pe}$ and of the geometrical parameters. Calculated dispersion characteristics $\beta = \beta(\omega, \bar{\omega}_{pe})$ have been previously reported (see e.g. Zakrzewski *et al* 1977, Moisan *et al* 1982). In general, these calculations agree rather well with the measurements, indicating that the errors caused by the neglect of the plasma radial inhomogeneity are small. This is to be expected provided $\beta a < 1$ (Trivelpiece 1967).

The attenuation coefficient is given by (see e.g. Bekefi 1966)

$$\alpha = \frac{1}{2}\frac{\mathrm{d}P_{abs}/\mathrm{d}z}{v_g W_t} \tag{2}$$

where v_g is the wave group velocity, W_t is the time-averaged total energy (i.e., magnetic + electric + kinetic energy of charged particles) per unit axial length, and $\mathrm{d}P_{abs}/\mathrm{d}z$ is the time-averaged absorbed power in the plasma per unit axial length. For $\nu_c \ll \omega$ the latter is given by (see e.g. Delcroix 1966)

$$\frac{\mathrm{d}P_{abs}}{\mathrm{d}z} = \int_0^a \frac{e^2}{2m}\left(\frac{E}{\omega}\right)^2 \nu_c n_e 2\pi r\,\mathrm{d}r = \frac{\bar{\nu}_c \varepsilon_0}{2}\left(\frac{\bar{\omega}_{pe}}{\omega}\right)^2 \int_0^a E^2 2\pi r\,\mathrm{d}r \tag{3}$$

where the second equality is for a radially homogeneous plasma characterised by the average quantities $\bar{\nu}_c$ and $\bar{\omega}_{pe}$. $E = (E_z^2 + E_r^2)^{1/2}$ is the wave electric field intensity, and ν_c is defined as in equation (14) of paper I. In a cold plasma, under low absorption conditions, the term $v_g W_t$ is equal to the total flow of electromagnetic energy across a plane perpendicular to the z axis, i.e., the total flux across this plane of the real component of the complex Poynting vector $\boldsymbol{E} \times \boldsymbol{H}^*/2$ ($\boldsymbol{E}$ and $\boldsymbol{H}$ are the complex field vectors, and the asterisk denotes complex conjugate).

Figure 1 shows calculated values of $\alpha\omega/\bar{\nu}_c$ versus $\bar{\omega}_{pe}/\omega$ for various values of the wave frequency and of the geometrical parameters (these results were kindly supplied by Dr Leprince and co-workers). It is to be noted that the attenuation is small at high electron densities, such that $\bar{\omega}_{pe} \gg \omega$, and becomes large close to the cut-off limit, i.e., when $\bar{\omega}_{pe}/\omega \rightarrow (1 + \varepsilon_g)^{1/2}$.

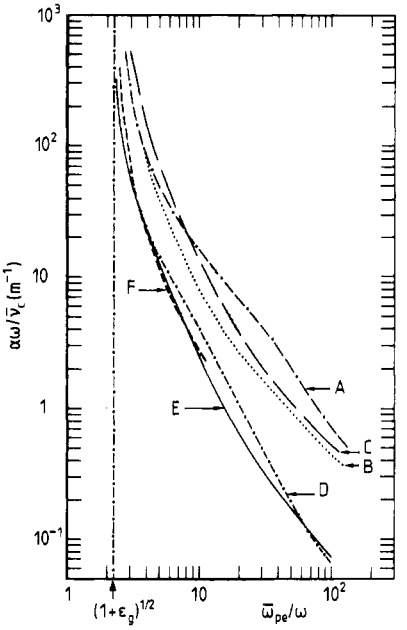

Figure 1. Calculated surface wave attenuation characteristics, assuming the plasma to be radially homogeneous, for different values of the wave frequency f in MHz and of the Pyrex glass tube ($\varepsilon_g = 4.52$) inside and outside radii, a and b in cm, respectively. Curves A and B: $f = 210$ and 2450 respectively, $a = 0.45$, $b = 0.60$. Curve C: $f = 2450$, $a = 0.30$, $b = 0.45$. Curves D, E and F: $f = 210$, 600 and 2450 respectively, $a = 1.25$, $b = 1.49$. The radius of the outer metallic waveguide is 2 cm in all cases.

The axial electron density distribution can also be derived semi-empirically from these equations (Glaude *et al* 1980). Equation (3) may be rewritten

$$\frac{dP_{abs}}{dz} = \theta\pi a^2 \bar{n}_e \tag{4}$$

where

$$\theta = \int_0^1 \frac{e^2\nu_c}{m}\left(\frac{E}{\omega}\right)^2 \frac{n_e}{\bar{n}_e} x\,dx = \frac{e^2\bar{\nu}_c}{m\omega^2}\int_0^1 E^2 x\,dx \tag{5}$$

represents the average absorbed power per electron. Here, $x = r/a$ and the second equality is again for a radially homogeneous plasma. Combining equations (2) and (4) we get

$$\bar{n}_e = \frac{2\alpha P_i}{\theta\pi a^2} \tag{6}$$

where $P_i = v_g W_t$ is the incident wave power at the abscissa z. The attenuation α is independent of the wave power. The quantity θ is also independent of P_i (this can be justified from the plasma balance, see below) but is a function of the operating parameters, i.e. wave frequency, gas pressure, and geometrical parameters, and also of $\bar{n}_e$ itself (at least in principle). Differentiating equation (6) and using again equation (2) one readily obtains

$$\frac{d\bar{n}_e}{dz} = -2\alpha\bar{n}_e\left(1 - \frac{\bar{n}_e}{\alpha}\frac{d\alpha}{d\bar{n}_e} + \frac{\bar{n}_e}{\theta}\frac{d\theta}{d\bar{n}_e}\right)^{-1}. \tag{7}$$

In previous work the heuristic assumption was made that the absorbed power in a plasma slice of length Δz is proportional to the number of electrons in this slice. On this assumption θ is independent of $\bar{n}_e$ and equations (6) and (7) together with the calculated attenuation characteristics suffice to determine the axial distribution of the electron density provided that θ and $\bar{\nu}_c$ may be estimated from the experiments. This semi-empirical approach was used by several workers (Glaude *et al* 1980, Chaker *et al* 1981, Nghiem *et al* 1982) and proved to be very satisfactory for the prediction of the axial properties of the plasma column as a function of the operating parameters. However, a complete theory must also provide the values of θ and $\bar{\nu}_c$. The radial theory of the plasma balance given in paper I provides these values as we now demonstrate.

2.2. *Plasma balance equations*

These equations were given and discussed in I but will be rewritten here under a somewhat different form that is more appropriate for the purposes of the present analysis. These equations are the following:

(i) Continuity and momentum transfer equations for the electrons and the ions:

$$\frac{1}{x}\frac{\mathrm{d}}{\mathrm{d}x}(nv_r x) = (Na)\,C_I n \tag{8}$$

$$v_r = \frac{D_e N}{Na}\left(\frac{e}{kT_e}\frac{\mathrm{d}\varphi}{\mathrm{d}x} - \frac{1}{n}\frac{\mathrm{d}n}{\mathrm{d}x}\right) \tag{9}$$

$$v_r\frac{\mathrm{d}v_r}{\mathrm{d}x} = -\frac{e}{M}\frac{\mathrm{d}\varphi}{\mathrm{d}x} - \frac{kT_i}{M}\frac{1}{n}\frac{\mathrm{d}n}{\mathrm{d}x} - Na\left(C_I + \frac{\nu_{in}}{N}\right)v_r \tag{10}$$

Here, $n = n_e = n_i$ is the plasma density, N is the neutral gas density, v_r is the radial drift velocity (identical for the electrons and the ions), C_I is the electron ionisation coefficient, D_e is the electron free diffusion coefficient, φ is the plasma potential, ν_{in} is an effective collision frequency for momentum transfer between ions and neutrals, M is the ion mass, and T_e and T_i are the electron and the ion temperatures, respectively.

(ii) Equations for the wave electric field in the plasma:

$$\frac{\mathrm{d}^2\mathscr{E}_z}{\mathrm{d}x^2} + \left(\frac{1}{x} + \frac{1}{\varepsilon_p}\frac{\mathrm{d}\varepsilon_p}{\mathrm{d}x}\frac{\beta^2}{\Gamma^2}\right)\frac{\mathrm{d}\mathscr{E}_z}{\mathrm{d}x} - (\Gamma a)^2\mathscr{E}_z = 0 \tag{11}$$

$$\mathscr{E}_r = \frac{\beta a}{(\Gamma a)^2}\frac{\mathrm{d}\mathscr{E}_z}{\mathrm{d}x}. \tag{12}$$

Here, $\mathscr{E}_z = E_z/E(0)$ and $\mathscr{E}_r = E_r/E(0)$ are the field components normalised to the field intensity at the axis $E(0)$, and Γ is defined by

$$\Gamma^2 = \beta^2 + \frac{\omega_{pe}^2 - \omega^2}{c^2} \tag{13}$$

where c is the velocity of light in vacuum.

(iii) Local power balance equation for the electrons:

$$\frac{e^2}{2m}\left(\frac{E}{\omega}\right)^2\nu_c = \frac{3m}{M}kT_e\nu_c + \sum_j eV_j NC_j + eV_I NC_I \tag{14}$$

where C_j is the electron rate coefficient for the excitation of the atomic level of potential energy V_j and V_I denotes the ionisation potential.

(iv) Absorbed power per unit axial length:

This is given by equation (4) in which θ is defined by the first equality in equation (5) (owing to the plasma radial inhomogeneity).

This set of equations allows the radial variations in the plasma parameters (e.g. plasma density, electron temperature, etc) and in the wave electric field intensity to be determined self-consistently. It further provides the dependence of $\bar{\nu}_c$ and of dP_{abs}/dz (and thus that of θ) on the various operating parameters, in particular the dependence of θ on $\bar{n}_e$ (see the results given in figures 10 and 15 in paper I).

3. Similarity laws

The numerical results given in I apply to the case $f = 600$ MHz, $a = 1.25$ cm, $b = 1.49$ cm, and it is interesting to look for simple similarity laws enabling the extension of these results, with no further calculations, to different operating conditions.

It is instructive to consider first the simple case of a radially homogeneous plasma column. In this case the solutions of equations (11) and (12) are

$$\mathscr{E}_z(z) = I_0(\Gamma a x)$$
$$\mathscr{E}_r(x) = \frac{\beta}{\Gamma} I_1(\Gamma a x) \tag{15}$$

where I_0 and I_1 are the zeroth and first-order modified Bessel functions, respectively. Figure 2 shows the variation of Γa and βa with $\bar{\omega}_{pe} a/c$ as obtained in this approximation for various values of the wave frequency and of the plasma radius. For $\bar{\omega}_{pe}^2 \gg \omega^2$ we have

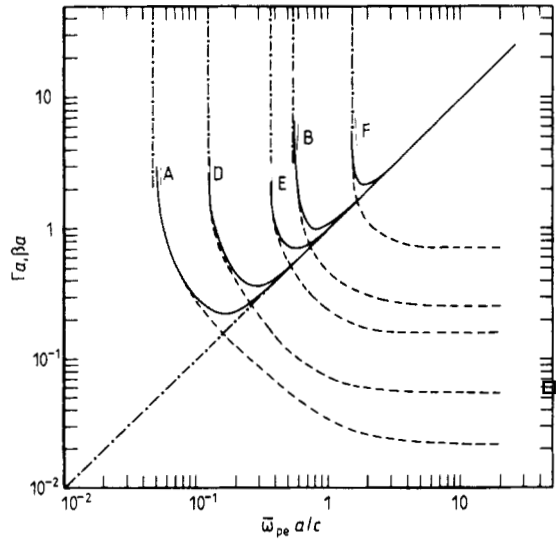

Figure 2. Calculated values of βa (dashed curves) and of Γa (full curves) versus $\bar{\omega}_{pe} a/c$ in the case of a radially homogeneous plasma. The labels of the different curves correspond to the same values of the operating parameters as in figure 1 (see caption to figure 1). The vertical chain lines indicate the cut-off values of $\bar{\omega}_{pe} a/c$.

$\Gamma \gg \beta$ and $\Gamma a \to \bar{\omega}_{pe} a/c$. In practice this limit is reached provided $\bar{\omega}_{pe}$ slightly exceeds the cut-off value $\bar{\omega}_{pec} = \omega(1 + \varepsilon_g)^{1/2}$. Close to the cut-off, i.e. for $\bar{\omega}_{pe} \to \bar{\omega}_{pec}$, we have $\Gamma \to \beta$ and both Γa and βa are large. However, in most practical situations the ratio $(\bar{\omega}_{pe}/\omega)^2$ is sufficiently large along a major portion of the plasma column so that $\Gamma a \to \bar{\omega}_{pe} a/c$ and $\Gamma \gg \beta$ everywhere, except axially at the end of the column and, radially, in the outer plasma layers close to the wall where n_e becomes small.

These conclusions may now be extended to the case of a radially inhomogeneous column. Provided $\bar{\omega}_{pe}^2 \gg \omega^2$ the equations (11) and (12) for the wave field may be simplified yielding

$$\frac{d^2\mathscr{E}_z}{dx^2} + \frac{1}{x}\frac{d\mathscr{E}_z}{dx} - \left(\frac{\bar{\omega}_{pe} a}{c}\right)^2 \frac{n_e}{\bar{n}_e}\mathscr{E}_z \approx 0 \tag{16}$$

$$\mathscr{E}_r \ll \mathscr{E}_z. \tag{17}$$

These equations constitute a good approximation almost everywhere in the column (except in the same regions as indicated above). With this simplification, inspection of the full set of radial equations reveals that $n_e(x)/\bar{n}_e$, $\mathscr{E}(x) \approx \mathscr{E}_z(x)$, $T_e(x)$, and $E(0)/\omega$ are functions only of the parameters Na and $\bar{\omega}_{pe} a/c$. This conclusion is very important as it allows the results given in I to be immediately extended to different combinations of the operating parameters. General results for argon can be obtained from the curves given in paper I provided the parameters p (gas pressure) and $\bar{n}_e$ used in that paper are replaced by the similarity parameters Na and $\bar{\omega}_{pe} a/c$.

As we have seen the link between the axial and the radial formulations summarised in §§ 2.1 and 2.2, respectively, is provided by the quantities θ and $\bar{\nu}_c$ and it is important to find out the similarity laws for these quantities. We first note that ν_c/N is a function only of T_e and that $T_e(x)$ is a function only of Na and $\bar{\omega}_{pe} a/c$. Hence

$$\frac{\bar{\nu}_c}{N} = f_\nu\left(\frac{\bar{\omega}_{pe} a}{c}, Na\right) \tag{18}$$

where f_ν is a function that can be derived from the results of paper I. In practice the dependence of $\bar{\nu}_c/N$ on $\bar{\omega}_{pe} a/c$ is relatively small (because $\bar{\nu}_c$ is a radially averaged value), therefore $\bar{\nu}_c/N \sim f_\nu(Na)$ as in a classical DC positive column.

Equations (3) and (5) may be rewritten

$$\frac{dP_{abs}}{dz} = \pi\varepsilon_0 c^2 N \left(\frac{\bar{\omega}_{pe} a}{c}\right)^2 \left(\frac{E(0)}{\omega}\right)^2 \int_0^1 \frac{\nu_c}{N}\mathscr{E}^2(x)\frac{n_e(x)}{\bar{n}_e} x\, dx \tag{19}$$

$$\frac{\theta}{N} = \frac{e^2}{m}\left(\frac{E(0)}{\omega}\right)^2 \int_0^1 \frac{\nu_c}{N}\mathscr{E}^2(x)\frac{n_e(x)}{\bar{n}_e} x\, dx \tag{20}$$

from which one may conclude that

$$\frac{dP_{abs}}{dz} = N f_P\left(\frac{\bar{\omega}_{pe} a}{c}, Na\right) \tag{21}$$

$$\theta = N f_\theta\left(\frac{\bar{\omega}_{pe} a}{c}, Na\right) \tag{22}$$

where the functions f_P and f_θ may be derived from the results given in figure 10 in paper I. A detailed analysis of these results reveals that θ has only a small variation with

$\bar{\omega}_{pe}a/c$ (except for $\bar{\omega}_{pe}$ close to the cut-off value) and satisfies very well the following similarity law

$$\theta \approx Nf_\theta(Na). \tag{23}$$

Thus, for most practical purposes, the assumption of θ being independent of $\bar{n}_e$ as used by other authors (Glaude *et al* 1980, Nghiem *et al* 1982) constitutes a satisfactory approximation. Note however that, strictly speaking, this assumption is not necessary in the framework of the present formulation. Indeed, the dependence of θ on $\bar{n}_e$ can be accounted for using equations (22) and (7) with no simplifications.

The similarity law expressed by equation (23) can also be derived in a more physical, though less rigorous way as shown in the appendix.

4. Application

Figure 3 shows calculated and experimental values of θ/p versus pa. The points are experimental data of Chaker *et al* (1981) for $f = 2450$ and 210 MHz, and $a = 0.45$ cm and 0.3 cm. The full curve was obtained from the results given in figure 10 in paper I (for

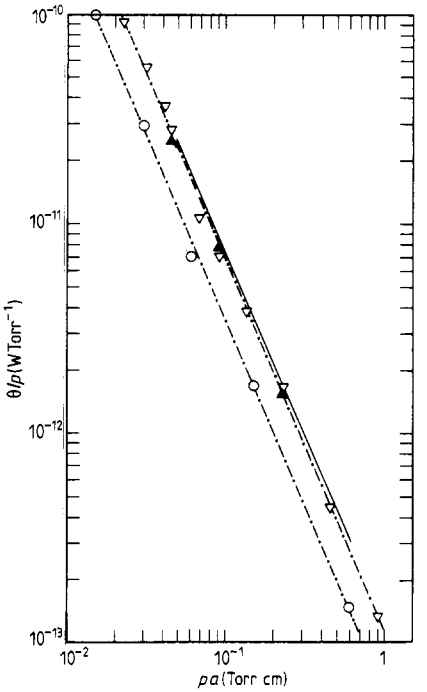

Figure 3. Average absorbed power per electron at unit gas pressure as a function of the pressure–radius product. Full curve: theory. The points are experimental data by Chaker *et al* (1981, 1982) for the following values of the wave frequency f in MHz and discharge tube ($\varepsilon_g = 4.52$) inside and outside radii, a and b in cm, respectively: (∇) $f = 2450$, $a = 0.45$, $b = 0.60$; ($\blacktriangle$) $f = 210$, $a = 0.45$, $b = 0.60$; ($\bigcirc$) $f = 2450$, $a = 0.30$, $b = 0.45$. The experimental data may be well fitted by straight lines as shown on the figure (dot-dashed lines).

$f = 600$ MHz, $a = 1.25$ cm) using the similarity law expressed by equation (23). For lack of information the gas temperature T_g was assumed to be 300 K. The predictions agree well with the measurements for $a = 0.45$ cm, $f = 2450$ and 210 MHz, but disagree

by about a factor of two with those for $a = 0.3$ cm, $f = 2450$ MHz (note however that the slopes of the theoretical and experimental curves are identical). These results seem to confirm that θ is independent of the wave frequency as expected from equation (23). The predicted dependence on the tube radius is verified only to within a factor of two and further measurements are necessary to test the accuracy of equation (23).

Theoretical and experimental values of $\bar{\nu}_c/p$ versus pa are compared in figure 4. The former were derived from the theoretical curve of $\bar{\nu}_c$ versus p given in figure 15 in I (calculated for $f = 600$ MHz, $a = 1.25$ cm, $T_g = 300$ K) using the similarity law $\bar{\nu}_c/N = f_\nu(Na)$. It is seen from figure 4 that this similarity law is satisfactorily confirmed by the various measurements for different wave frequencies and tube radii.

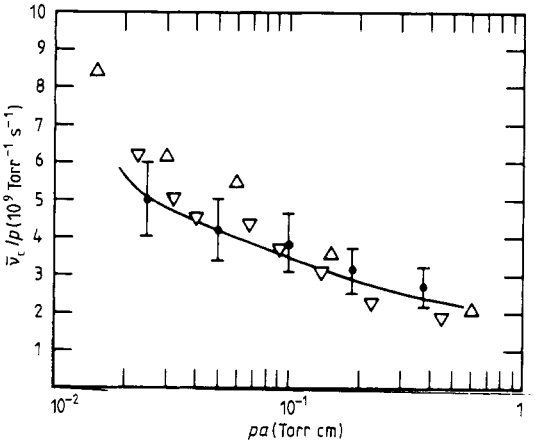

Figure 4. Effective collision frequency for momentum transfer between electrons and neutrals at unit gas pressure as a function of the pressure–radius product. Full curve: theory. Experimental data: (●) $f = 360$ MHz, $a = 1.25$ cm, $b = 1.49$ cm (Glaude *et al* 1980); (▽) $f = 2450$ MHz, $a = 0.45$ cm, $b = 0.60$ cm; (△) $f = 2450$ MHz, $a = 0.30$ cm, $b = 0.45$ cm (Chaker *et al* 1982).

The axial distribution of the electron density may now be determined from equations (6) and (7) using the theoretical values of θ and α. These equations could be integrated numerically but it is interesting to make some approximations providing simple, closed formulas for the distribution $\bar{n}_e(z)$ and for the length of the plasma column as a function of the operating parameters. As shown in figure 1 the variation of $\lg(\alpha\omega/\bar{\nu}_c)$ is approximately linear with $\lg(\bar{\omega}_{pe}/\omega)$ except in the range of $\bar{\omega}_{pe}/\omega$ close to the cut-off (which corresponds to the end of the plasma column). Therefore, we will use the approximation

$$\alpha\frac{\omega}{\bar{\nu}_c} = g(\omega, a)\left(\frac{\bar{\omega}_{pe}}{\omega}\right)^{-k} \tag{24}$$

where $g(\omega, a)$ and k are determined by fitting equation (24) to the curves given in figure 1. This approximation is satisfactory for $\omega_{pe} \gg \bar{\omega}$, i.e., the same range where the simple similarity laws derived in § 3 are expected to apply.

Using equation (24) the integration of equation (7) is straightforward (neglecting the variation of θ with $\bar{n}_e$) and yields

$$\frac{\bar{n}_e(z)}{\bar{n}_e(0)} = \left(1 - \frac{k}{1 + (k/2)}\,\alpha_0 z\right)^{2/k} \tag{25}$$

where α_0 is the value of the attenuation at $z = 0$. Here, the axial distance z is measured from the launcher. The initial values $\bar{n}_e(0)$ and α_0 are fully determined by equation (6), the attenuation curves given in figure 1, and the theoretical values of θ and $\bar{\nu}_c$, for given operating conditions (ω, p, geometrical parameters, and incident power at $z = 0$).

The length of the plasma column L may be approximately determined from equation (25) using the end condition $\bar{n}_e(L) = \bar{n}_{ec}$, where $\bar{n}_{ec}$ is the cut-off value of the electron density. Hence, one readily obtains

$$L = \frac{1 + (k/2)}{k} \frac{1}{\alpha_0} \left[1 - \left(\frac{\bar{\omega}_{pec}}{\bar{\omega}_{pe}(0)} \right)^k \right] = \frac{1 + (k/2)}{k} \frac{1}{\alpha_0} \left[1 - \left(\frac{1 + \varepsilon_g}{y_0} \right)^{k/2} \right] \tag{26}$$

where $y_0 = (\bar{\omega}_{pe}(0)/\omega)^2$.

Equation (25) becomes inaccurate towards the end of the column, therefore equation (26) is approximate. Nevertheless, this simple theoretical description predicts very accurately the axial distribution of the electron density and the influence of the different operating parameters on the length of the column. Figure 5 shows calculated and

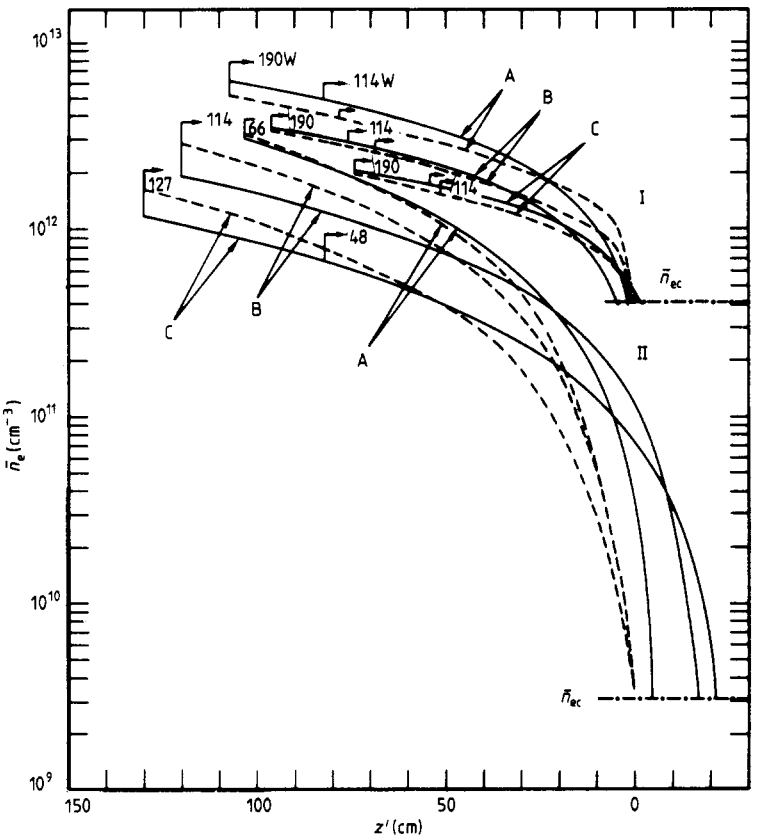

Figure 5. Calculated (full curves) and measured (dashed curves) axial distributions of the electron density for different values of the wave frequency f in MHz (curves I, $f = 2450$; curves II, $f = 210$), wave incident power in W, and pressure p in Torr (A) $p = 0.5$, (B) $p = 0.2$, (C) $p = 0.1$). The abscissa scale is the axial distance measured from the end of the column ($z' = 0$ corresponds to the point where the column was experimentally observed to end). The symbol (Γ) indicates the initial value of the electron density and the plasma length corresponding to a given incident HF power.

measured axial distributions of the electron density for different values of the wave frequency, gas pressure and incident power (for $a = 0.45$ cm, $b = 0.60$ cm, $d = 2$ cm, $\varepsilon_g = 4.52$). The discrepancies between theory and experiment become significant only at the end of the column (note the definition of the abscissa scale given in the caption), especially for $f = 210$ MHz. In this case however, the low-attenuation conditions are barely satisfied as $\omega/\bar{\nu}_c$ reaches values as low as about 2. More accurate calculations of the end portion of the column could be performed without resorting to the approximation (24), i.e., taking into account the correct behaviour of the attenuation close to the cut-off.

5. Conclusion

The model of a low-pressure plasma column sustained by a weakly damped surface wave presented here is an improvement over other theoretical descriptions previously reported. The present model takes into account the coupling between the plasma maintenance conditions and the surface wave propagation characteristics, thus providing a complete theoretical description of the whole system in which both the radial and the axial variations in the plasma properties are considered.

Simple similarity laws were proved to exist for this system provided the radially averaged electron plasma frequency is somewhat larger than the cut-off value $\omega_{pec} = \omega(1 + \varepsilon_g)^{1/2}$, this condition being satisfied along practically the whole plasma column in most practical situations. Indeed, we have shown that the radial distributions of the plasma density, electron temperature, and wave-electric field intensity, as well as the ratio of the magnitude of this field at the axis to the wave angular frequency, $E(0)/\omega$, are functions only of the similarity parameters $\bar{\omega}_{pe}a/c$ and Na, where $\bar{\omega}_{pe}$ is the electron plasma angular frequency corresponding to the radially averaged electron density $\bar{n}_e$, N is the neutral gas density, a is the discharge tube inside radius, and c is the velocity of light in vacuum. From here we have been able to show that θ/N and $\bar{\nu}_c/N$, where θ is the average absorbed power per electron and $\bar{\nu}_c$ is the radially averaged electron–neutral collision frequency for momentum transfer, are functions only of those two similarity parameters. However, the dependence of θ/N and $\bar{\nu}_c/N$ on $\bar{\omega}_{pe}a/c$ is small and these quantities are essentially determined by the values of the Na-product. These similarity laws enable the extension of the numerical results reported previously to different operating conditions with no further calculations.

Moreover, analytical expressions were derived for the axial distribution of the electron density $\bar{n}_e(z)$ and for the length of the plasma column L as a function of the operating parameters. The calculations were shown to agree well with available experimental data. Therefore we conclude that the present model gives an accurate physical description of this type of discharge.

Acknowledgments

The author wishes to thank Dr P Leprince and his co-workers for supplying the calculations of the surface wave wave-number and attenuation coefficient used in this work, and for valuable discussions. I am also indebted to Professor M Moisan for revising the first version of the manuscript. Acknowledgment is made to the Centre National de la Recherche Scientifique for the award of a Visiting Fellowship.

Appendix

For the low pressures of interest in this work elastic losses may be neglected in the local power balance for the electrons (see I), thus equation (14) may be written approximately

$$\frac{e^2}{2m}\left(\frac{E}{\omega}\right)^2 \nu_c = eV_I(1+\gamma)\,\nu_I \tag{A1}$$

where $\nu_I = NC_I$ is the ionisation frequency, and $\gamma = \sum_j V_j C_j / V_I C_I$.

Using equation (A1) and neglecting the variation of γ with radius the absorbed power in the plasma per unit axial length may be rewritten

$$\frac{dP_{abs}}{dz} = eV_I(1+\gamma)\int_0^a n_e \nu_I 2\pi r\, dr \simeq eV_I(1+\gamma)\,\pi a^2 \bar{n}_e \bar{\nu}_I \tag{A2}$$

where $\bar{\nu}_I$ represents an effective average value of the ionisation frequency. Using the continuity equation (8) dP_{abs}/dz can also be written

$$\frac{dP_{abs}}{dz} = eV_I(1+\gamma)\int_0^a \frac{1}{r}\frac{d}{dr}(n_e v_r r)\,2\pi r\, dr = eV_I(1+\gamma)\,2\pi a n_e(a)\, v_r(a) \tag{A3}$$

where $v_r(a)$ is the radial velocity of the electrons and ions at the plasma–sheath boundary. As shown in I, $v_r(a)$ is equal to the local isothermal ion sound speed, i.e., $v_r(a) \sim [kT_e(a)/M]^{1/2}$.

Equating the expressions (A2) and (A3) yields

$$\bar{\nu}_I = \bar{\nu}_W \tag{A4}$$

where

$$\bar{\nu}_W = \frac{2}{a}\frac{n_e(a)}{\bar{n}_e} v_r(a) \tag{A5}$$

represents an average frequency for the loss of electrons to the wall. Therefore, equation (A4) represents the steady-state maintenance condition of the plasma column.

Using equations (A2) and (A4) the parameter θ (defined by equation (4)) can also be written

$$\theta = eV_I(1+\gamma)\,\bar{\nu}_I = eV_I(1+\gamma)\,\bar{\nu}_W. \tag{A6}$$

Thus, $\theta/\bar{\nu}_I$ represents the average energy necessary to produce an electron–ion pair in the discharge.

In the theory of the classical DC positive column the loss of the electrons to the wall is generally expressed in terms of an effective electron diffusion coefficient D_{se} (Allis and Rose 1954, Muller and Phelps 1980) such that

$$\bar{\nu}_W = D_{se}/\Lambda^2 \tag{A7}$$

where Λ is the diffusion length for the discharge tube ($\Lambda = a/2.405$ for infinite cylindrical geometry). Introducing such an effective diffusion coefficient for the present case equation (A6) may be rewritten

$$\frac{\theta}{N} = eV_I(1+\gamma)\frac{D_{se}}{N\Lambda^2} = eV_I(1+\gamma)\frac{D_{se}}{\bar{D}_e}\frac{\bar{D}_e N}{(N\Lambda)^2} \tag{A8}$$

where $\bar{D}_e$ is the radially averaged electron free diffusion coefficient.

In a classical isothermal, quasineutral positive column at low pressures the quantities D_{se}/D_e and D_eN are only a function of $N\Lambda$ (thus of Na). In the surface wave produced plasma the electron temperature increases slightly with the radius and this causes some changes in the radial profiles of the plasma density in comparison with those of a classical DC positive column (see I). Nevertheless the basic creation and loss processes are essentially the same in both situations, and the average values of the electron temperature in the surface wave plasma are close to those of the positive column for the same pressure–radius product (see, e.g., Chaker *et al* 1982 and paper I). Therefore, we can expect the right-hand term in equation (A8) to also be mainly a function of Na in the surface wave plasma, and hence the similarity law

$$\theta/N \approx f_\theta(Na) \tag{A9}$$

to be approximately verified.

References

Aliev Yu M, Boev A G and Shivarova A P 1982 *Phys. Lett.* **92** 235–7

Allis W P and Rose D J 1954 *Phys. Rev.* **93** 84–93

Bekefi G 1966 *Radiation Processes in Plasmas* (New York: Wiley)

Chaker M, Nghiem P, Bloyet E, Leprince P and Marec J 1981 *Rapport Interne L.P. 190, Université de Paris-Sud (Orsay)*

—— 1982 *J. Physique-Lett.* **43** L71–L75

Delcroix J L 1966 *Physique des Plasmas* Vol 2 (Paris: Dunod)

Ferreira C M 1981 *J. Phys. D: Appl. Phys.* **14** 1811–30

Glaude V M M, Moisan M, Pantel R, Leprince P and Marec J 1980 *J. Appl. Phys.* **51** 5693–8

Moisan M, Beaudry C and Leprince P 1975 *IEEE Trans. Plasma Sci.* **PS-3** 55–9

Moisan M, Ferreira C M, Hajlaoui Y, Henry D, Hubert J, Pantel R, Ricard A and Zakrzewski Z 1982 *Rev. Phys. Appl.* **17** 707–27

Moisan M, Pantel R, Hubert J, Bloyet E, Leprince P, Marec J and Ricard A 1979a *J. Microwave Power* **14** 57–61

Moisan M, Pantel R, Ricard A, Glaude V M M, Leprince P and Allis W P 1980 *Rev. Phys. Appl.* **15** 1383–97

Moisan M, Zakrzewski Z and Pantel R 1979b *J. Phys. D: Appl. Phys.* **12** 219

Muller III C H and Phelps A V 1981 *J. Appl. Phys.* **51** 6141–8

Nghiem P, Chaker M, Bloyet E, Leprince P and Marec J 1982 *J. Appl. Phys.* **53** 2920–2

Trivelpiece A W 1967 *Slow-Wave Propagation in Plasma Waveguides* (San Francisco: San Francisco University Press)

Zakrzewski Z, Moisan M, Glaude V M M, Beaudry C and Leprince P 1977 *Plasma Phys.* **19** 77–83

Note added in proof

Recent experimental determinations of the average absorbed power per electron, θ, in an argon plasma sustained by a surface microwave in various capillary tubes with different diameters (Dervisevic E, Bloyet E, Laporte C, Leprince P, Marec J, Pouey M and Saada S, *Proc. XVIth Int. Conf. Phenomena in Ionized Gases, Düsseldorf, FRG* at press) have shown that the theoretical similarity law of θ/p versus pa derived in this paper is remarkably well confirmed by the experiments.

An equation for the axial electron density distribution similar to equation (25) of the present paper was also recently derived by Z Zakrzewski (1983 *J. Phys D: Appl. Phys.* **16** 171–80).